BIBECHANA
Vol. 22, No. 3, December 2025, 223-236

ISSN 2091-0762 (Print), 2382-5340 (Online)
Journal homepage: http://nepjol.info/index.php/BIBECHANA
Publisher:Dept. of Phys., Mahendra Morang A. M. Campus (Tribhuvan University)Biratnagar

Advancement of plant-based inhibitor acquired from Elaeocarpus aungustifolius Blume leaves to control carbon steel corrosion in simulated concrete pore solution

**Madhab Gautam[1,2], Dhruba Babu Subedi[1], Yuvraj Paudel[1]
Kamal T. Kunwar Magar[1], Nootan Prasad Bhattarai[1,*], Jagadeesh Bhattarai[1,*]**

[1] *Central Department of Chemistry, Tribhuvan University, Kirtipur 44618, Kathmandu, Nepal*
[2] *Department of Chemistry, Tribhuvan M. Campus, Tribhuvan University, Tansen 32500, Palpa, Nepal*
*Corresponding author. Email: bhattarai_05@yahoo.com[JB], neutan08@gmail.com[NPB]

Abstract

The extraordinary compressive strength of concrete makes it one of the most popular building materials, second only to water. However, early reinforcement corrosion is a common problem with concrete structures reinforced with carbon steel (CS). This issue underscores the significance of understanding corrosion-retarding systems that incorporate inhibitors. This research evaluates the effectiveness of leaf extract from Elaeocarpus angustifolius *Blume (LEEA) as an inhibitor in an aqueous saturated calcium hydroxide electrolyte that simulates a concrete pore solution (SCPS) with a pH level exceeding 11.5. The objective is to evaluate the corrosion-inhibiting capacity of LEEA at 500-4000 ppm in SCPS to reduce the corrosion of reinforcing carbon steel (RCS) at 298K over four months or more using gravimetric weight loss (GrWL) and electrochemical polarization (ECP) techniques. GrWL and ECP methods yielded the maximal inhibition efficiencies of 93.9% and 81.7%, respectively, at 4000 ppm LEEA in SCPS. The results of ECP experiments demonstrated that the corrosion current density (CCD) decreased with increasing LEEA concentrations. This observation indicates that LEEA exhibits a significant inhibitory effect in the SCPS environments. Phyto-compounds (PCs), including polyphenols, alkaloids, and flavonoids found in LEEA, can inhibit both cathodic and anodic (i.e., mixed) processes by promoting the best-fitting Langmuir adsorption isotherm model on the RCS surface. Surface analyses confirmed the corrosion-inhibiting effectiveness of LEEA in enhancing concrete's anti-corrosion properties through a protective layer on RCS.*

Keywords
Corrosion-resistant film, phyto-inhibitor, polarization, reinforcement corrosion, polarization.

Article information
Manuscript received: April 28, 2025; Revised July 28, 2025; Accepted: August 3, 2025
DOI https://doi.org/10.3126/bibechana.v22i3.78028

1 Introduction

The most widespread structural building material is reinforcement concrete because of its affordability, mechanical strength, and adaptability [1]. The reinforcement concrete structures' durability is affected by their alkaline nature of interspersed pore solution, which has a pH of around 12-14 [2]. As a result, cement paste's hydration produces a thin, passive, and stable oxide film [3] that firmly sticks to the RCS surface to prevent early corrosion deterioration. The RCS corrosion deterioration describes the premature degradation of reinforced concrete structures caused by electrochemical processes on the CS surface brought on by ambient dampness, high temperatures, carbonated conditions, and the ingress of vicious ions such as sulfates and chlorides [4]. It is the most prevalent issue in hostile (urban or industrial) and coastal environments [5]. Corrosion causes concrete structures to crack, spall, and weaken, which causes reinforced concrete foundations to collapse too soon [6].

The reinforcement corrosion presents significant challenges and should be managed effectively in time [7]. Synthetic waterproofing compounds are utilized for long periods as preventive concrete admixtures to mitigate corrosion of RCS [8]. Unfortunately, a considerable number of these synthetic compounds have the potential to harm living beings and contribute to environmental contamination [9]. It underscores the viability of utilizing plant-based green extracts as an alternative approach for corrosion prevention in reinforcement concrete infrastructures [10]. Secondary metabolites such as alkaloids, phenols, flavonoids, and others derived from plant waste—encompassing leaves, roots, stems, and bark—are particularly relevant in this context. These compounds exhibit distinctive aromatic systems, unsaturated -systems, and lone pairs of electrons associated with heteroatoms [11]. Such characteristics facilitate the formation of physical and chemical adsorption layers that disrupt corrosion reactions at the interface between corroded RCS and the concrete mix that incorporates plant extracts, thereby demonstrating significant corrosion-inhibiting properties [12].

Nepal ranked the world's second-richest country in forest resources after Brazil, and is home to a diverse range of flora and fauna [13]. However, many forest products in Nepal have been underutilized. Research into their potential as environmentally friendly corrosion inhibitors for reinforced concrete (ReC) is still in its early stages. Some studies have documented the use of Nepalese plant-based corrosion inhibitors to control the corrosion of mild steel (MS) in various electrolytes. For instance, the leaves of *Callistemon citrinus* have been tested on MS in NaCl [14], while extracts from *Areca catechu* and *Laurus nobilis* have been studied in a 0.5M NaCl solution [15]. Additionally, *Aegle marmelos* has shown effectiveness on MS in bioethanol [16], and a range of plants including *Acacia catechu*, *Terminalia arjuna*, *Aegle marmelos*, *Catharanthus roseus*, *Callistemon citrinus*, and *Laurus nobilis* have all been evaluated on MS in acidic electrolytes [17].

Researchers have also explored *Vitex negundo* on aluminum and copper in biodiesel and its blends [18]. Further studies have involved *Aegle marmelos* and *Catharanthus roseus* in both bioethanol and its blends [16], extracts of *Vitex negundo* and *Catharanthus roseus* on MS for waterproofing applications [11], and the stem extract of *Tinospora cordifolia* on aluminum and copper in biodiesel-based fuels [19]. More recent studies have examined leaf extracts of *Mangifera indica* [20] and *Psidium guajava* [21] on MS in concrete beams and slabs. Ongoing efforts continue to identify new and effective green inhibitors for ReC infrastructure, including the endemic plant species *Elaeocarpus angustifolius* Blume from Nepal, as a potential green inhibitor.

In this context, it is meaningful to mention herein that in the domain of materials science, two synthetic and commercial waterproofing agents, along with the methanolic extract of *Mangifera indica* leaves, had exhibited notable anti-corrosion properties, thereby warranting their recommendation for the protection of reinforced mild steel (RMS) infrastructures [20]. The corrosion resistance of 1000 and 2000 ppm concentrations of *M. indica* extracts applied to RMS within concrete surpasses that of equivalent concentrations of the commercial waterproofing agents. This enhanced performance was evidenced by shifts in half-cell potential (HCP) values toward more noble directions (i.e., < 10 % corrosion probability regions). Such findings suggest that plant-based anti-corrosive concrete admixtures may provide greater advantages than the utilization of conventional waterproofing chemicals [20]. Hence, this study aimed to present a rationale for the integration of plant-derived metabolites from *Elaeocarpus angustifolius* Blume leaf as effective anti-corrosive additives in ferroconcrete formulations.

Elaeocarpus angustifolius Blume, commonly known as the bead tree or rudraksha, is a well-known medicinal plant recognized for its various pharmacological and ethno-medicinal properties [22]. The name comes from Greek, where "carpus" means fruit and "eleaeo" refers to olive, which reflects the olive-like appearance of the tree's fruits [22]. The *Elaeocarpus* family includes over 360 species worldwide, with 26 species identified in Nepal alone [16]. Among these, *E. angustifolius* Blume—also referred to as *Elaeocarpus ganitrus* Roxburgh and *E. sphaericus* Gaertner—is an

evergreen tree notable for its ornamental, stony endocarp, known as Rudraksha [23]. According to Hindu mythology, the Rudraksha tree has sprouted from the tears of Lord Shiva, and its fully developed blue fruits are often referred to as "blueberry beads" [24].

The rudraksha tree is a large, evergreen, deciduous tree with a spreading crown that can grow to 50 and 200 feet [25]. Its leaves are simple, alternate, and oblong-lanceolate, measuring 10-15 cm long. The underside of the leaves has a dull, fibrous texture, while the upper surface is bright green [26]. This tree is well-known for its spiritual and therapeutic benefits, as it produces beads with segmented ridges, believed to possess electromagnetic properties capable of dispelling negative energy [27]. Research indicates that methanolic leaf extracts of the rudraksha tree (*E. ganitrus*) exhibit significant analgesic effects and contain alkaloids, tannins, and flavonoids [28]. Additionally, methanolic leaf extracts of *E. sphaericus* are rich in phytoconstituents such as saponins, alkaloids, phenols, flavonoids, sterols, and carbohydrates; however, they do not contain amino acids or proteins [29].

Because the leaves of this medicinal plant have a high phenol and flavonoid content and contain many classes of bioactive secondary metabolites, the bioactivity tests showed that the leaves might be a potential source of antibacterial, antibiotic, antioxidant, anti-diabetic medications [30], and other purposes like as anti-corrosive agents. However, a considerable quantity of leaves from this plant acts as debris without deriving any industrial or monetary benefits. While a limited number of studies have underscored the corrosion-inhibitory properties of the leaf extract [16] and seed extract [31] in aggressive electrolytes, there has yet to be an investigation into their efficacy in mitigating corrosion in ReC. According to what we know, the methanolic leaf extract from the *Elaeocarpus aungustifolius* Blume plant was not considered a corrosion inhibitor for reinforced carbon steel in SCPS/reinforcement concrete in literature, which is why the present research is considered novel.

Therefore, this study aims to evaluate the effectiveness of leaf extracts from the *Elaeocarpus angustifolius* Blume plant (LEEA) as environmentally friendly corrosion inhibitors in simulated concrete pore solutions (SCPS) with a pH level higher than 11.5. The primary objective is to assess the viability of LEEA as a green corrosion inhibitor within this context. The research investigates the ability of LEEA to reduce the corrosion of carbon steel (CS) in SCPS utilizing gravimetric weight loss (GrWL) and potentiodynamic polarization (PoP) methods. The findings may contribute to plant-derived green inhibitors designed to mitigate corrosion in concrete reinforcement.

2 Materials and Method

AR grade methanol and calcium carbonate were employed for the preparation of LEEA and saturated $Ca(OH)_2$ solution, respectively. They were with a purity of 98%. *Elaeocarpus aungustifolius* Blume leaves, as illustrated in Fig. 1(a), were identified with voucher code RDP-01 and deposited at the Department of Plant, National Herbarium and Plant Laboratory in Godavari, Lalitpur, after being collected from the Tribhuvan University Campus premises close to the Central Department of Environmental Sciences, TU-Kirtipur, Nepal. The collected leaves were placed in a shady area until completely dried and ground in an electric grinder to make leaf powder, as in Fig. 1(b). About 400 grams of leaf powder of *Elaeocarpus aungustifolius* Blume were taken in 2000 mL conical flasks with 800 mL of methanol, as described elsewhere [32]. After being tightly sealed in the conical flask and thoroughly shaken, they were kept for 2 weeks or more with regular shaking, as shown in Fig. 1(c). Following the shaking procedure, the supernatant mixtures were kept for a few hours to separate the supernatant using filtration. Excess methanol in the filtrate was removed using a rotary evaporator (IKA®RV 10 digital V, Germany) and water bath at 40°C, as illustrated in Fig. 1(d). Then, the semi-solid leaf extract of *Elaeocarpus aungustifolius* Blume (LEEA) was stored at 4°C. The saturated calcium hydroxide [$Ca(OH)_2$] solution, with a pH of approximately 12±0.5, was used to prepare the SCPS.

Figure 1: Photos illustrating the different stages of the LEEA preparation: leaves of *Elaeocarpus aungustifolius* plant (a), dried leaves powder (b), leaf-powder dipped in CH_3OH (c), and a solvent evaporator machine (d).

For the GrWL approach, fifteen thermo-mechanically treated carbon steel (CS) specimens, designated as 500CS (NBS marked 500 XD series), were meticulously prepared. As previously outlined in other studies, the surface preparation involved using silicon carbide paper with grits ranging from 200 to 2000 [15]. The average diameter and length of each of the 500CS pieces were 1.13 cm and 2 cm, respectively. A 5-digit micro-balance (BM-252; A&D Weighing Co., Japan) with an accuracy of

0.00001 grams was initially used to record carefully the weight of each 500CS piece (abbreviated as W_0). The composition (wt.%) of the 500CS pieces is roughly 98% Fe, with trace C, Mn, S, and P, as described elsewhere [33].

Out of the 15 sample pieces, three 500CS pieces were immersed in three 100 mL beakers containing 50 mL of SCPS without LEEA (controlled SCPS). Similarly, twelve 500CS pieces were dipped in twelve beakers containing 50 mL SCPS with 500-4000 ppm LEEA for 2802 hours to estimate the corrosion rate (CoR). For this, the weight of each 500CS specimen after being exposed to it for t times (indicated as W_t) was recorded after 7, 14, 28, 43, 60, 90, and 117-day immersion in each SCPS variant. The corrosion rate (CoR) for each sample in the SCPS with LEEA concentrations ranging from 500 to 4000 ppm and in the SCPS without LEEA (control SCPS) was calculated using the formula provided in equation (1), as described elsewhere [34]. Additionally, the estimated surface coverage () and corrosion inhibition efficiency [CoIE) were calculated using equations (2) and (3), respectively, as given in Ref. [35].

$$CoR(mm/y) = \frac{\Delta W\ (g)\ \times\ 87600}{A\ (cm^2)\times\ \rho\ (gcm^{-2})\times t\ (hrs.)} \quad (1)$$

$$\theta\ = \frac{CR_{(control)}\ -\ CR_{(LEEA)}}{CR_{(control)}} \quad (2)$$

$$\%\ \text{CoIE} = \frac{\text{CR}_{(\text{control})}\ -\ \text{CR}_{(\text{LEEA})}}{\text{CR}_{(\text{control})}} \times 100 \quad (3)$$

Where, $W = W_o\text{-}W_t$

Furthermore, electrochemical analysis was performed through potentiodynamic polarization (PoP) experiments using an Iquant 64 potentiostat (Model No.: IFC 101-32240) with a three-electrode system, as outlined in the literature [36]. The slopes of the anodic and cathodic polarization curves, derived from formulas (4) and (5), were used to calculate the corrosion potential (E_{cor}), corrosion current density (i_{cor}), the corrosion rate (CoR) based on i_{cor} or weight loss, and the corrosion inhibition effectiveness (CoIE) based on i_{cor} and weight loss [37]. Consequently, i_{cor}-based CoR was determined using Tafel plots of both the anodic and cathodic curves [38].

$$\text{CR}_{(\text{icor})} = 0.13 \times i_{cor} \times \frac{E}{\rho} \quad (4)$$

$$\%\text{InE(icor)} = \frac{\text{icor}_{(\text{control})}\text{-icor}_{(\text{LEEA})}}{\text{icor}_{(\text{control})}} \times 100 \quad (5)$$

Where, $= 7.86\ g/cm^3$, is density and E = 55.85, equivalent weight of 500CS pieces.

The inhibitory activity of the phyto-compounds (PCs) from LEEA is demonstrated using Langmuir adsorption isotherm [39, 40]. The linear fit plot of this isotherm allows us to estimate G_{ads}, using equation (6), as illustrated in literature [41].

$$\frac{C_{LEEA}}{} = \frac{1}{K_{ads}} + C_{LEEA} \quad (6)$$

In this case, K_{ads} = adsorption equilibrium constant, which helps determine the free energy change of adsorption (G_{ads}) value, as described in previous literature [42].

The phytochemical tests [32, 43] of LEEA were conducted to decide the presence (+) or absence () of various phytochemicals in LEEA. The FTIR spectra were recorded in the wavenumber range of 400-4000 cm^1 using the ATR mode (IR Affinity-1S, Shimadzu Corp., Japan) to confirm the presence of functional groups in LEEA in addition to the phytochemical tests. PCs with their electronic properties identified using UV-Vis spectra recorded by a UV-Visible spectrophotometer (SPECORD®200 PLUS, Germany) across the wavelength range of 200 to 800 nm. Furthermore, a high-performance quadrupole time-of-flight mass spectrometer (XEVO G2-XS QTOF, IIT Ropar, Punjab, India) was employed to identify the distinct PCs in LEEA through liquid chromatography-mass spectrometry (LC-MS, Waters Corp., USA).

The study examined the morphological and compositional modifications of the 500CS samples behind 2802 hours in control-SCPS and SCPS with 500 to 4000 ppm LEEA, using a scanning electron microscope (SEM-Thermo Fisher Scios Field Emission, USA, 10 kV), equipped with energy-dispersive X-ray spectroscopy (EDAX Octane Elect EDS/EDX detector, USA, 30 kV). It captured the surface images of the 500CS pieces submerged in control SCPS and SCPS with 500-4000 ppm LEEA using white light interferometry (WLI) with a NewView-9000 from Zygo Corp.

3 Results and Discussion

The phytochemical tests confirmed that phenols, flavonoids, alkaloids, terpenes, saponins, glycosides, and carbohydrates are present in the LEEA as the main PCs, as summarized in Table 1, constituted heteroatoms and unsaturated electrons and/or aromatic compounds [28]. These findings align with existing literature [30]. The PCs from LEEA contribute to forming a diffusion-barrier passive layer on the surface of immersed 500CS pieces through the adsorption phenomenon, which aids in controlling corrosion and is consistent with previous studies [44].

The UV-Vis analysis revealed distinct peaks associated with various functional groups of LEEA-PCs, thereby confirming the electronic transitions present in the extract, as illustrated in Fig. 2(a). The UV-Vis spectra of LEEA show absorption peaks at 472 nm, 503 nm, 535 nm, 606 nm, and 664 nm, suggesting the existence of aromatic or conjugated unsaturated systems [45]. Previous study reported that the UV-Vis peaks at 472 nm and 535 nm indicated the presence of terpenoids [46]. The peaks at 606 nm and 664 nm are identified as chlorophyll [47]. Consequently, PBEs exhibit a strong anti-corrosive effect due to their richness in secondary metabolites (SMs). However, UV-Vis anal-

ysis presents challenges in identifying specific constituents corresponding to these absorption peaks [48]. Therefore, it is essential to complement UV-Vis findings with other analytical techniques [49], such as FTIR, GC/MS, or UHPLC/MS, to characterize the plant extracts, as discussed in the next sections.

Table 1: Tests for phyto-compounds (PCs) in LEEA

PCs	Result	PCs	Result
Alkaloid	++	Saponin	+
Phenol	+++	Tanine	−
Flavonoid	++	Terpenoid	++
Glycoside	+	Carbohydrate	−

Note: Signs +, ++, +++ indicate abundance, while the sign − indicates absence.

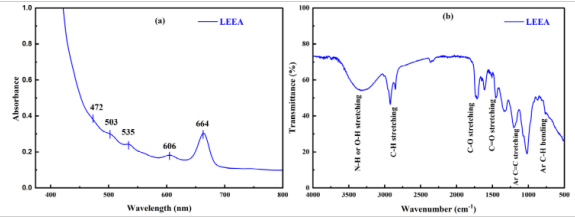

Figure 2: (a) UV-Vis and (b) FT-IR spectrum of LEEA.

The results of functional groups, as shown in Fig. 2(b), are confirmed in the PCs of LEEA by FTIR analysis. The presence of nitrogen (N), sulfur (S), and oxygen (O) heteroatoms and functional groups like phenols, carboxylic acids, and amines, distinguished by their abundance and degree of unsaturation was verified by FTIR spectra's values [50]. Phenolic, alcoholic or amines compounds are indicated by a peak at 3345 cm^1, which correspond to the O-H or N-H stretching vibrations found in aromatic compounds [51]. An FTIR peak at 2922 reflects the asymmetric stretching of C-H vibrations. Other notable peaks include those associated with carbonyl C=O groups at 1708 cm^1 and C=O or C=C stretching at 1605 cm^1 [52], as well as C=C-C aromatic stretching at 1456 cm^1 [53]. These findings signify the presence of various functional groups, including alcohols, amines, ketones, acids, and unsaturated compounds.

Furthermore, peaks ranging from 1260 to 1380 cm^1 confirm that all plant extracts contain aromatic rings [54, 55]. A significant peak at 1200 cm^1 indicates C-N stretching vibrations, suggesting the presence of secondary or tertiary amines in the LEEA [56]. Moreover, a peak at 1020 cm^1 corresponds to O-H or C-H bending vibrations in aromatic compounds [57]. These findings are consistent with prior studies [58]. Therefore, the results of the FTIR analyses support the potential application of the LEEA as an effective anticorrosive admixture in concrete formulations to mitigate the corrosion of reinforcement.

The FTIR analysis confirms the presence of diverse functional groups in the examined LEEA, enhancing our understanding of its chemical composition. These groups are responsible for inhibiting the corrosion of reinforcement metals in concrete infrastructures. Using mass bank matching, the LC-MS analysis of the LEEA reported eight PCs mainly, including phenols, terpenoids, alkaloids, and flavonoid functional groups. These anticipated PCs, which assumed to be present in the extract are listed in Table 2 and shown in Fig. 3, are verified from phytochemical testing, UV-Vis, FTIR, and LC-MS analyses.

Table 2: Major compounds present in LEEA analyzed from LC-MS analysis

S.N.	Retention Time (min)	Molecular Formula & Weight (g/mol)	Name of Compounds	Types of Compounds
1	1.853	$C_{18}H_{17}NO_3$ (295.1)	DP-Oxazole Acid	Alkaloids
2	4.238	$C_{12}H_{18}ClNO_2S$ (275.1)	Dimethenamid	Alkaloid
3	4.864	$C_{21}H_{22}O_{10}$ (432.4)	Apigenin-7-O-glucoside	Flavonoids
4	5.219	$C_{21}H_{20}O_{11}$ (448.1)	Kaempferol-3-O-glucoside	Flavonoid
5	5.659	$C_{30}H_{52}O$ (428.7)	Epifriedelanol	Terpenoids
6	6.149	$C_{20}H_{21}NO_4$ (339.1)	Canadine or Papaverine	Alkaloid
7	8.000	$C_{15}H_{12}O_3$ (240.1)	4'-Hydroxyflavone	Flavonoid
8	9.498	$C_{15}H_{11}O_6^+$ (287.2)	Cyanidin	Flavonoid

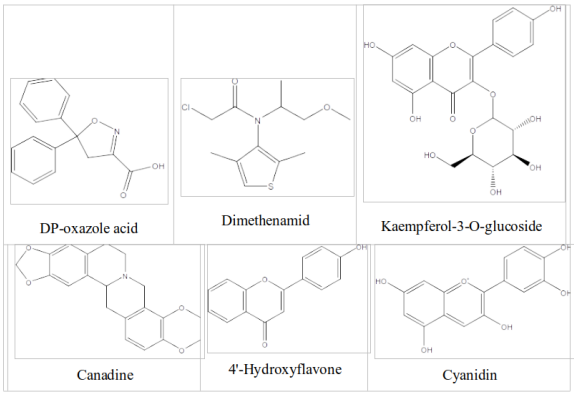

Figure 3: Structural formula of PCs assumed to be present in LEEA identified with LC-MS technique.

These studies demonstrated that LEEA has a potent anti-corrosive impact on concrete reinforcement corrosion. It allows the chemicals in LEEA to attach to the CS specimens dipped in SCPS, either physically through weak interactions like Van der Waal interactions and/or chemically through ionic or co-covalent bonding [59].

The corrosion rate (CoR) of immersed CS in both control SCPS and SCPS with LEEA concentrations was estimated using the weight loss method, and the results are plotted in Fig. 4(a). The CoR of the CS in SCPS with 1000 ppm LEEA is lower than that in the control SCPS with 500 and 2000-4000 ppm LEEA, indicating that LEEA effectively inhibits the corrosion of CS in SCPS with 1000 ppm LEEA. As shown in Fig. 4(a), the CoR of sample specimens immersed in SCPS containing 500, 2000, and 4000 ppm of LEEA ranged from 0.0013 to 0.0069 mm/y. In contrast, the CoR in SCPS with 400 ppm LEEA was approximately 0.0017 mm/y. The 1000 ppm LEEA addition to the SCPS displayed the highest corrosion resistance. Consequently, the corrosion-inhibiting efficiency was about 95% in the SCPS with 1000 ppm LEEA, as illustrated in Fig. 4(b). It demonstrates the enhanced corrosion inhibition effect of 1000 ppm LEEA in SCPS.

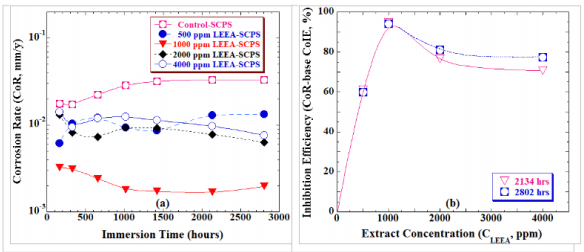

Figure 4: Variations of CoR (a) and CoIE (b) of CS immersed in SCPS without (control) and with 500-4000 ppm LEEA.

These findings indicate the formation of a stable and anti-corrosive passive film at the 1000 ppm LEEA concentration, in contrast to the other concentrations of 500, 2000, and 4000 ppm LEEA. Also, it might be a result of the formation of a persistent adsorption layer. Over time, more phytocompounds (PCs)-based inhibitor molecules may have been adsorbed onto the CS surface, which could cause the extract to desorb somewhat from the CS surface [60]. The dissolution of PCs adsorbed from LEEA inhibitors in the SCPS by the generation of a chelate between the iron atoms of CS pieces and the heteroatoms of phytoconstituents present in LEEA inhibitor may be the cause of the decrease negligibly in inhibition for 2802 hours immersion [61].

The corrosion inhibition of CS specimens enriched with increasing amounts of LEEA. The instability of the CS specimen in the control SCPS, which does not contain LEEA, may be attributed to the break of early-formed layers of CS across the metal-layer interface. This detachment can increase the corrosion rate over extended immersion times [62]. The lower CoR of CS in SCPS containing LEEA concentrations ranging from 1000 to 4000 ppm is due to beneficial phytochemicals such as polyphenols, alkaloids, and flavonoids in LEEA. These compounds facilitate the formation of a thin passive coating film on the surface of 500CS through the adsorption of complex polyphenols or heteroaromatic chemicals [63].

According to qualitative examinations, the LEEA retains a variety of flavonoids, alkaloids, phenols, and terpenoids. The PCs function as key parts of the phyto-molecular interactions with the corroded surfaces of CS specimens in the SCPS, elucidated by the adsorption isotherm model, such as the Langmuir isotherm. The molecular interaction between the corroded CS and PCs of LEEA is due to heteroatoms and highly conjugated aromatic - electrons in the PCs [64]. Overall, the use of LEEA as a promising inhibitor for CS in SCPS at different immersion times, as demonstrated by the stabilization of the highly concentrated extract to the SCPS.

Langmuir adsorption isotherm, illustrated in Fig. 5 is utilized to investigate the adsorption of LEEA's PCs onto the CS piece in SCPS across various immersion periods. It assessed the corrosion inhibition mechanism of LEEA on rusty CS specimens in SCPS with changing LEEA concentrations. It is meaningful to mention herein that for the linear Langmuir isotherm plot, the estimated CoR was based on the gravimetric weight loss (GrWtL) method. Figure 5 shows a linear relationship with a very high coefficient of determination (R^2) that tends to unity. However, the slope is not equal to one (i.e., 1.284-1.431), indicating a fit not only to the Langmuir monolayer adsorption isotherm. In corrosion inhibition studies, the standard adsorp-

tion Gibbs energy is frequently estimated through linear regression of the Langmuir isotherm, as outlined in equation (6).

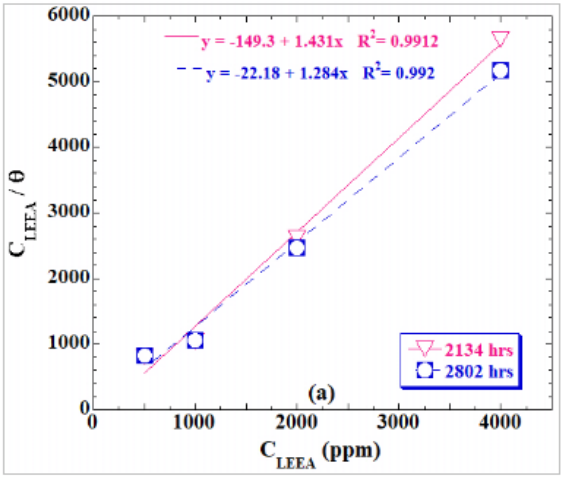

Figure 5: Langmuir isotherm plots for CS specimens in SCPS with different concentrations of LEEA at different immersion times.

In this adsorption isotherm model, the slopes of the corresponding straight lines must adhere to the requirements of the Langmuir isotherm, which stipulates a slope of unity. This theoretical framework enables relatively precise estimations of the standard adsorption Gibbs energy based on experimentally determined surface coverage. However, a deviation in the slope from unity to values ranging from 1.284 to 1.431, as illustrated in Fig. 5, suggests non-Langmuir adsorption phenomena, which may indicate the presence of multi-site adsorption or surface heterogeneity [65]. Additionally, the thermodynamic analysis, based on G°_{ads} values, suggests that the adsorption in this condition is spontaneous and involves electrostatic interactions, characteristic of physisorption [66]. The negative values of G°_{ads} further support the favorable spontaneous nature of the adsorption process of PCs on the immersed CS surface. We have tested other adsorption isotherm models like Temkin, El-Awady, and Freudlich adsorption models [67]. They did not fit with R^2 values comparatively much lower than that of the Langmuir isotherm plots. Consequently, the Langmuir adsorption isotherm demonstrates the best fit compared with the Temkin isotherm. These outcomes align with conclusions from earlier research notifying identical adsorption behaviors of PCs on corroded steel specimens in acidic environments [66].

Based on the experimental results from weight loss tests, as discussed above, the corrosion inhibition efficiency and mechanism of LEEA adsorption onto corroded carbon steel (CS) have already been investigated. Besides, the corrosion inhibition kinetics of LEEA on the CS surface in SCPS, both with and without LEEA, can be examined using potentiodynamic polarization (PoP) analysis. The corrosion potential (E_{cor}) values shifted to more negative (cathodic) directions without significant changes in anodic current density as a function of LEEA concentrations, as depicted in Fig. 6. In addition, the cathodic current density (i_{cath}) and corrosion current density (i_{cor}) decreased with LEEA concentrations in SCPS, indicating the suppression of cathodic reactions on CS in the given conditions, even though there is no consistent shifting of E_{cor}. These electrochemical properties are rendered by a protective passive film formation on the surface of the corroded CS in the SCPS with 500-4000 ppm LEEA.

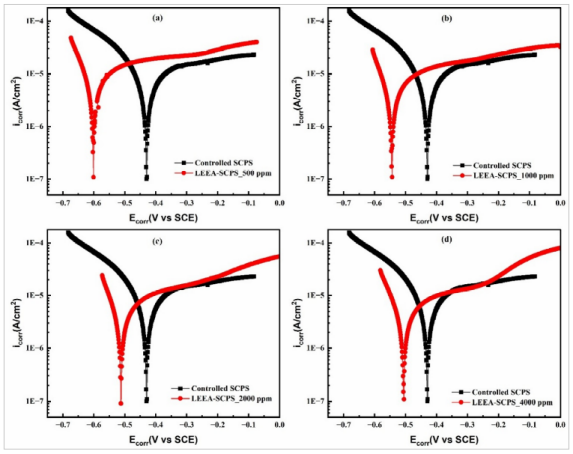

Figure 6: Plots obtained PoP for CS immersed in SCPS with (a) 500 ppm, (b) 1000 ppm, (c) 2000 ppm, and (d) 4000 ppm LEEA including control SCPS.

The corrosion rate and inhibition efficiency were determined using the corrosion potential (E_{cor}), corrosion current (i_{cor}), and Tafel slopes of the anode ($_{anod}$) and cathode ($_{cath}$) from potentiodynamic polarization (POP) curves through the Tafel extrapolation method, as shown in Fig. 6 and also summarizes in Table 3. Increases in $_{aond}$ and $_{cath}$, driven by LEEA in SCPS, indicate improved polarization resistance (R_p) predominantly by cathodic reduction reactions. A higher $_{cath}$ suggests hindered reduction processes, while an increased $_{anod}$ points to slower CS dissolution and potential passivation [68].

Table 3: Corrosion current (i_{cor}) and inhibition efficiency (icor-based/GrWtL-based CorIE) calculations for CS immersed in SCPS without and with 500–4000 ppm LEEA, obtained from GrWL and PoP approaches

LEEA (ppm)	E_{cor} (mV)	i_{cor} (A/cm^2)	β_{anod} (mV/dec)	β_{cath} (mV/dec)	R_{pol} (kΩ·cm^2)	i_{cor}-based CorIE (%)	GrWtL-based CorIE (%)
Blank	-428.4	7.301	2.54	6.33	0.04	–	–
500	-596.1	3.808	9.58	14.67	2.06	47.8	59.9
1000	-545.2	2.576	7.86	17.83	3.22	64.7	94.1
2000	-512.1	1.946	11.09	18.89	7.43	73.4	81.1
4000	-507.4	1.569	12.29	17.39	9.31	78.5	77.3

Ultimately, this trend reflects the formation of a passive layer, enhanced R_p, and decreased corrosion rates [69]. In literature, the CoIEs of 4000 ppm leaf extracts of *Tagetes erecta* [37] *Ziziphus budhensis* [33], and *Sisamum indica* [46] were 73.78%, 81.48%, and 81.7% (i_{cor}-based), and 67.81%, 91.22%, and 93.9% (GrWL-based), respectively. In contrast, a 4000 ppm LEEA exhibited inhibition efficiencies of 81.7% (i_{cor}-based) and 93.9% (GrWL-based), indicating the LEEA has shown almost the same corrosion-inhibiting efficiency for reinforced concrete as other plant extracts reported in the literature.

We investigated the morphological changes of CS sample surfaces after a 2802-hour immersion in SCPS with 4000 ppm of LEEA, compared to SCPS under control conditions. The CS specimen immersed in control SCPS exhibited a severely corroded surface with several corrosion-related flaws, as shown in Fig. 7(a). The significant corrosion observed was due to the prolonged exposure to the control SCPS, which facilitated the interaction of hostile ions with the CS surface through existing surface flaws [70]. In contrast, the SEM micrographs of the pieces immersed for the same duration in SCPS containing 4000 ppm of LEEA, shown in Fig. 7(b), displayed LEEA's remarkable anti-corrosive effectiveness. The samples have smooth surfaces with minimal corrosion-related flaws and few corrosion products. The protective adsorption layers, created by LEEA, act as a barrier against hostile ions, reducing their ability to penetrate the surface [71].

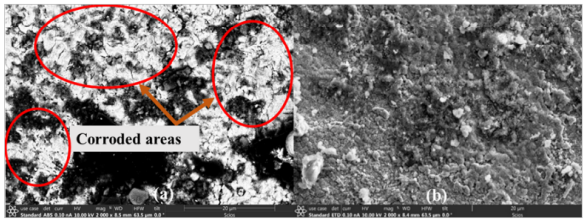

Figure 7: SEM micrograph for the adsorption layer formed over CS pieces after immersion for 2802 hours in (a) control SCPS and (b) SCPS with 4000 ppm LEEA.

The EDS examination demonstrated a notable decrease in Fe from 98.37% to 61.69% in the CS sample at control-SCPS after 2802 hours, alongside an increase in O-content to 33.13%, indicating significant corrosion product formation. Conversely, samples with 4000 ppm LEEA for 2802 hours at SCPS displayed reduced corrosion, with 72.63% Fe and 22.38% O, as shown in Table 4. These results align with Verma and Khan [72], demonstrating minimal rust formation and corrosion-resistant properties on the CS surface. Thus, LEEA effectively inhibits iron dissolution in SCPS, acting as a corrosion-preventive agent.

Table 4: EDX elemental analysis of immersed CS pieces in control SCPS and SCPS with 4000 ppm LEEA after 2802 hours immersion

Specimens	Fe (wt.%)	O (wt.%)	Ca (wt.%)	Si (wt.%)	Misc. (wt.%)
Fresh CS specimen	98.37	–	0.17	0.40	1.08
CS immersed for 2802 hrs in control SCPS	61.69	33.13	3.34	1.84	–
CS immersed for 2802 hrs in SCPS with 4000 ppm LEEA	72.63	22.38	3.12	1.87	–

The white light interferometry (WLI) technique, known for its high sensitivity in corrosion studies, was employed to assess surface roughness and morphology. This method provides rapid and accurate three-dimensional (3D) and 2D topographic analysis of corroded metal surfaces, offering precise lateral and vertical resolution without physical contact [73]. Figures 8(a) and 8(b) display the 2D and 3D profiles of the CS specimens after 2802 hours of immersion in 2000 ppm LEEA at SCPS. The surface roughness (SR) measured 7.059 m, lower than the 8.510 m recorded for specimens immersed in SCPS without the plant extract [33]. It represents a 17.05% reduction in surface roughness when LEEA is present, indicating its effectiveness in minimizing corrosion [74]. These results are consistent with SEM analysis, further confirming the superior performance of LEEA as a corrosion inhibitor for immersed CS samples.

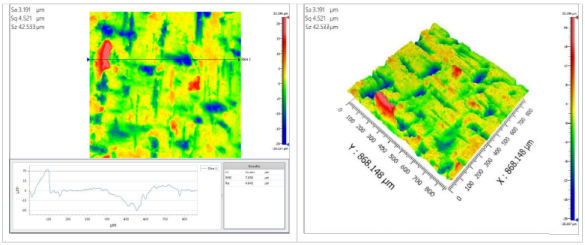

Figure 8: 2D and 3D WLI images of the CS specimen after immersion for 2802 hrs in SCPS with 2000 ppm LEEA.

The results show LLEA has strong corrosion-inhibiting properties in SCPS environments typical of reinforced concrete, supported by SEM/EDS and WLI assessments. A graphical representation (Fig. 9) to elucidate the corrosion-inhibiting mechanism attributed to the adsorption of plant-derived PCs from LLEA on CS in SCPS, both in the absence of the inhibitor (control) and with concentrations of LLEA ranging from 500 to 4000 ppm under ambient conditions. This illustration aims to clarify the distinguished inhibiting effect of LLEA within SCPS or concrete environments, as demonstrated in Fig. 9, by following the steps below.

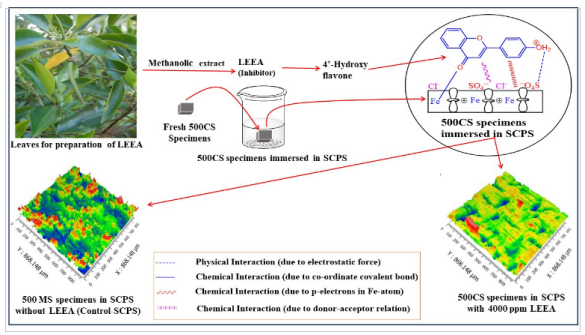

Figure 9: A diagrammatic representation shows the adsorption mechanism of 4'-hydroxyflavone onto 500CS in SCPS with 2000 ppm LEEA at ambient conditions.

i. The electrostatic interaction occurs between protonated PCs of LEEA and the positively charged Fe^{2+} ions from CS, facilitating physical adsorption [75].

ii. Coordination bonding between lone pairs (non-bonding electrons) on hetero-atoms like O or N in PCs and the unoccupied d-orbitals of Fe-atoms in the immersed CS specimens may result in chemical adsorption [41].

iii. The aromatic ring and the empty d-orbitals of the Fe-atoms in the RCS interact with -electrons to facilitate chemical adsorption [44].

iv. The d-electrons of Fe-atoms of corroded CS specimens and the vacant anti-bonding molecular orbitals of the PCs components of LEEA undergo chemical adsorption, resulting in donor-acceptor interactions or retro-donation [36].

The analysis of multiple adsorption sites indicates that the phytochemicals (PCs) obtained from the LEEA are suitable for forming a passive adsorption layer on the surface of CS specimens, serving effectively as corrosion inhibitors. This study explores the plant-based inhibitors for the first time in concrete admixtures to prevent the corrosion of CS in SCPS, highlighting their environmentally friendly properties.

4 Conclusions

This study demonstrates that first-time use of LEEA effectively prevents the corrosion of CS specimens in simulated concrete pore solution (SCPS). Results from gravimetric weight loss (GrWL), potentiodynamic polarization (PoP), and surface analysis like SEM/EDS and WLI confirm the formation of a protective surface layer that slows down the corrosion rate of 500CS in SCPS containing 500-4000 ppm LEEA as a concrete admixture. The optimal inhibition efficiencies achieved were 93.9% (measured by GrWL) and 78.5% (measured by PoP) at 4000 ppm LEEA in SCPS at room temperature. The PoP measurements indicate that the cathodic reaction primarily governs the effectiveness of LEEA as a significant corrosion inhibitor. The Langmuir adsorption isotherm suggests that the LEEA-based PCs create a homogeneous, single-layer protective coating on the surface of the corroded CS through physical adsorption.

This study established that the initial application of LEEA significantly mitigates the CS specimens when exposed to SCPS. The findings obtained from GWL, PoP, and surface analysis techniques-SEM/EDS and WLI confirm the formation of a protective surface layer. This layer effectively reduces the corrosion rate of 500-grade carbon steel (500CS) within LEEA concentrations ranging from 500 nd 4000 ppm at SCPS, as a concrete admixture. The maximum inhibition efficiencies recorded were 93.9% (as determined by GWL) and 78.5% (as determined by PoP) at a concentration of 4000 ppm LEEA in SCPS at ambient temperature. Additionally, the PoP measurements suggest that the cathodic reaction predominantly influences the efficacy of LEEA as a corrosion inhibitor for concrete environments.

Furthermore, the Langmuir adsorption isotherm indicates that LEEA-based protective coatings form a uniform, single-layer protective film on the

surface of corroded carbon steel through physical adsorption. Compared to the 500CS sample immersed in controlled SCPS without LEEA, surface analysis using SEM/EDS and WLI revealed that the surface of the CS remained smooth after immersion for about four months or more in LEEA at SCPS. The extract (500-4000 ppm LEEA) is derived from the leaves of *Elaeocarpus angustifolius*, which are typically discarded and thus readily available at minimal or no cost. It not only ensures cost-effectiveness but also promotes environmental sustainability. The non-toxic and eco-friendly nature of the extract enhances its suitability for large-scale applications in real-world infrastructure without posing any risks.

Acknowledgments

The authors acknowledge Mr. Madhusudan Dhakal (IMR-CAS in Shenyang, China) for arranging WLI and Dr. M.A. Fickenscher (University of Cincinnati, USA) for providing SEM/EDS facilities. The authors also thank Mr. R.D. Pandey for his assistance in identifying plant species and preparing LEEA. MG acknowledges the University Grant Commission (UGC-Nepal) for awarding his Ph.D. research grants (Award No.: PhD-78/79-S&T-03).

Author contributions

MG, NPB & JB planned the experimentations; specimen preparation, practical works, and data examination by MG, DBS, YRP, and KTKM; analyzed the data and results overview by MG, NPB, and JB; documented the manuscript draft by MG and NPB, and did the conclusive edits by MG and JB. All authors read and consented to the final manuscript.

Conflict of interest

The authors assert that they hold no conflicts of interest

Data availability statement

Upon appeal, the corresponding author(s) will supply data to reinforce their conclusions.

References

[1] S.S. Ubayi, A. Ahmad, E. Ahmad, B.S. Abubakar, S. Dulawat, M. Nuhu, U.S. Ibrahim, and A. Ibrahim. A review on the impact of jute fiber reinforcement on mechanical properties of concrete. *International Journal of Engineering Science*, 1:13–34, 2024.

[2] S. Yousuf, P. Shafigh, and Z. Ibrahim. The ph of cement-based materials: A review. *Journal of Wuhan University of Technology-Materials Science Edition*, 35(5):908–924, 2020.

[3] D. Wang, Y. Wang, J. Wang, K. Ma, C. Dai, J. Wang, and F. Pan. Corrosion resistance of mg-al-zn magnesium alloy concrete formwork in portland cement paste. *Construction and Building Materials*, 325(4):126745, 2022.

[4] A.F.A. Fuhaid and A. Niaz. Carbonation and corrosion problems in reinforced concrete structures. *Buildings*, 12(5):586, 2022.

[5] A. Castañeda Valdes, F. Corvo Perez, I. Pech Pech, R. Marrero Águila, and E. Bastidas-Arteaga. Durability requirements for reinforced concrete structures placed in a hostile tropical coastal environment. *Buildings*, 14(8):2494, 2024.

[6] A.K.J. Thales and K. Sadeghi. Causes and effects of structural cracks. *International Journal of Modern Trends in Science and Technology*, 8(2):64–69, 2022.

[7] M.A. Quraishi, D.K. Nayak, R. Kumar, and V. Kumar. Corrosion of reinforced steel in concrete and its control: An overview. *Journal of Steel Structures and Construction*, 3(1), 2017.

[8] M. Whittaker and L. Heine. Toxicological and environmental issues associated with waterproofing and water repellent formulations. In *Waterproof and Water Repellent Textiles and Clothing*. 2018.

[9] Shehnazdeep and B. Pradhan. A study on effectiveness of inorganic and organic corrosion inhibitors on rebar corrosion in concrete: A review. *Materials Today: Proceedings*, 65(4), 2022.

[10] M. Sheydaei. The use of plant extracts as green corrosion inhibitors: A review. *Surfaces*, 7(2):380–403, 2024.

[11] J. Bhattarai, M. Somai, N. Acharya, A. Giri, A. Roka, and N. P. Phulara. Study on the effects of green-based plant extracts and waterproofers as anti-corrosion agents for steel-reinforced concrete slabs. *E3S Web Conf.*, 302:02018, 2021.

[12] K. Bijapur, V. Molahalli, A. Shetty, A. Toghan, P. De Padova, and G. Hegde. Recent trends and progress in corrosion inhibitors and electrochemical evaluation. *Applied Sciences*, 13(18):10107, 2023.

[13] R. K. Khanal. Forest resources potential for economic growth of nepal. *Voice: A Biannual Bilingual Journal*, 16(2):61–78, 2024.

[14] J. Bhattarai, M. Rana, M. R. Bhattarai, and S. Joshi. Effect of green corrosion inhibitor of callistemon plant extract on the corrosion behavior of mild steel in nacl and hcl solutions. In *CORECON 2016 Proceedings*, 2016. Publication of NIGIS/NACE, Paper No. MI-17, pp. 1-8.

[15] M. Rana, S. Joshi, and J. Bhattarai. Extract of different plants of nepalese origin as green corrosion inhibitor for mild steel in 0.5 m nacl solution. *Asian Journal of Chemistry*, 29(5):1130–1134, 2017.

[16] P. Katuwal, R. Regmi, S. Joshi, and J. Bhattarai. Assessment on the effective green-based nepal origin plants extract as corrosion inhibitor for mild steel in bioethanol and its blend. *European Journal of Advanced Chemical Research*, 1(5), 2020.

[17] J. Bhattarai, M. Rana, M. R. Bhattarai, R. Regmi, and S. Joshi. Effect of green corrosion inhibitor of nepalese origin plants for corrosion control of mild steel in aggressive environments. In *CORECON 2018 Proceedings*, 2018. Publication of NIGIS/NACE, Paper No. MCI-17, p. 12.

[18] B. N. Subedi, K. Amgain, S. Joshi, and J. Bhattarai. Green approach to corrosion inhibition effect of vitex negundo leaf extract on aluminum and copper metals in biodiesel and its blend. *International Journal of Corrosion Scale Inhibition*, 8(3):744–759, 2019.

[19] K. Amagain, B. N. Subedi, S. Joshi, and J. Bhattarai. A comparative study of the anticorrosive response of tinospora cordifolia stem extract for al and cu in biodiesel-based fuels. *E3S Web Conf.*, 355:01005, 2022.

[20] M. Somai, A. Giri, A. Roka, and J. Bhattarai. Comparative studies on the anti-corrosive action of waterproofing agent and plant extract to steel rebar. *Macromolecular Symposia*, 410(1):2100276, 2023.

[21] A. Roka, M. Gautam, A. Giri, N.P. Bhattarai, and J. Bhattarai. The anti-degradation consequences of water repellent-based inhibitors for controlling mild steel corrosion in concrete composite. *E3S Web Conf.*, 455:01002, 2023.

[22] Z. Banu, R. Poduri, and S. Bhattamisra. A comprehensive review on phytochemistry, health benefits, and therapeutic potential of elaeocarpus angustifolius blume. *Annals of Phytomedicine - International Journal*, 13(1):370–383, 2024.

[23] S. Hardainiyan, B.C. Nandy, and K. Kumar. Elaeocarpus ganitrus (rudraksha): A reservoir plant with their pharmacological effects. *International Journal of Pharmaceutical Sciences Review and Research*, 34(1):55–64, 2015.

[24] R. Lamichhane, D. Gautam, M.S. Miya, H.B. Chhetri, and S. Timilsina. Role of non-timber forest products in national economy: A case of jajarkot district, nepal. *Grassroots Journal of Natural Resources*, 4(1):93–105, 2021.

[25] M.S. Miya, S. Timilsina, and A. Chhetri. Ethnomedicinal uses of plants by major ethnic groups of hilly districts in nepal: A review. *Journal of Medicinal Botany*, 4:24–37, 2020.

[26] P. Manu, A. Lal, and R. Anju. Elaeocarpus sphaericus: A tree with curative powers: An overview. *Research Journal of Medicinal Plant*, 7:23–31, 2013.

[27] P. Aryal. Medicinal value of elaeocarpus sphaericus: A review. *Asian Journal of Pharmacognosy*, 6(3):15–21, 2021.

[28] N.Z.W. Kiromah, M. Chondrosuro, and Y. Krisdiyanti. Ethanol and methanol extract of analgesic activities of ganitri leaves (elaeocarpus ganitrus roxb) for in vivo. *Journal of Fundamental and Applied Pharmaceutical Sciences*, 2(1):53–58, 2021.

[29] D. Kumar, A. Sanghi, R. Chandra, S. Arora, and A. Kumar. Membrane stabilizing and antioxidant activities of extracts from leaves of elaeocarpus sphaericus. *International Journal of ChemTech Research*, 10(6):668–673, 2021.

[30] S. Joshi, S. Amatya, R.D. Pandey, P. Khadka, and J. Bhattarai. Antimicrobial, antioxidant, antidiabetic, cytotoxic activities and gc-ms analysis of methanolic extract of elaeocarpus sphaericus leaves from nepal. *International Journal of Advanced Research in Chemical Sciences*, 8(1):11–23, 2021.

[31] N. Raghavendra and B.E. Kumaraswamy. Elaeocarpus seed extraction and their impact as a corrosion inhibitor for mild steel submerged in hcl wash solution: Insight from experimental, mathematical, and theoretical views. *Journal of Failure Analysis and Prevention*, 21:1096, 2021.

[32] M. Gautam, D.B. Subedi, J. Dhungana, N.P. Bhattarai, and J. Bhattarai. Utilization of bark extract of phyllanthus emblica as a sustainable corrosion inhibitor to reinforced concrete infrastructures in aggressive environments. *E3S Web Conf.*, 610:03002, 2025.

[33] M. Gautam, N.P. Bhattarai, and J. Bhattarai. Leaf-based extracts of nepal origin plants as efficient inhibitors for controlling rebar corrosion in concrete pore solution. *International Journal of Corrosion Scale Inhibition*, 13(4):2087–2111, 2024.

[34] P. Magrati, D.B. Subedi, D.B. Pokharel, and J. Bhattarai. Appraisal of different inorganic inhibitors action on the corrosion control mechanism of mild steel in hno3 solution. *Journal of Nepal Chemical Society*, 41(1):64–73, 2020.

[35] D.B. Pokharel, D.B. Subedi, and J. Bhattarai. Study the effect of sodium nitrite as a green corrosion inhibitor for the sputter-deposited tungsten-based ternary alloys in 0.5 m nacl solution. *Bibechana*, 12:1–12, 2015.

[36] M. Gautam, N.P. Bhattarai, and J. Bhattarai. Sesamum indicum leaf extract as environmentally benign inhibitor to mitigate mild steel corrosion in cement pore solution. *Journal of Institute of Science and Technology*, 30(1):101–113, 2025.

[37] M. Gautam, N.P. Bhattarai, and J. Bhattarai. Gravimetric and electrochemical interpretation of plant extract as corrosion inhibitor for embedded-steel in concrete pore solution. In *Proceedings of 10th International Conference (CONSEC2024)*, pages 784–792, Chennai, Madras, India, 2024.

[38] ASTM International. Astm g102-89: Standard practice for calculation of corrosion rates and related information from electrochemical measurements. pages 416–422, 1989. ASTM Standard.

[39] I. Langmuir. The constitution and fundamental properties of solids and liquids: Part i-solid. *Journal of the American Chemical Society*, 38(11):2221–2295, 1916.

[40] M.I. Temkin. Adsorption equilibrium and the kinetics of processes on non-homogeneous surfaces and in the interaction between adsorbed molecules. *Zhurnal Fizicheskoi Khimii*, 15:296–332, 1941.

[41] A. Zakeri, E. Bahmani, and A.S.R. Aghdam. Plant extracts as sustainable and green corrosion inhibitors for protection of ferrous metals in corrosive media: A mini review. *Corrosion Communications*, 5:25–38, 2022.

[42] H. Ren, Y. Liu, Z. Gong, B. Tan, H. Deng, J. Xiong, R. Marzouki, et al. Pumpkin leaf extract crop waste as a new degradable and environmentally friendly corrosion inhibitor. *Langmuir*, 40(11):5738–5752, 2024.

[43] S.Y. Keskin, A. Avcı, and H.F.F. Kurnia. Analyses of phytochemical compounds in the flowers and leaves of spiraea japonica var. fortunei using uv-vis, ftir, and lc-ms techniques. *Heliyon*, 10(3):e25496, 2024.

[44] Q. Ma, Q. Yang, J. Zhang, F. Ren, C. Xia, and F. Chen. Anti-corrosion properties of bio-inspired surfaces: a systematic review of recent research developments. *Materials Advances*, 5:2689–2718, 2024.

[45] M. Taniguchi and J.S. Lindsey. Database of absorption and fluorescence spectra of >300 common compounds for use in photochem cad. *Photochemistry and Photobiology*, 94:290–327, 2018.

[46] M. Saxena and J. Saxena. Evaluation of phytoconstituents of acorus calamus by ftir and uv-vis spectroscopic analysis. *International Journal of Biological and Pharmaceutical Research*, 3(3):498–501, 2012.

[47] X.E. Mabasa, L.M. Mathomu, N.E. Madala, E.M. Musie, and M.T. Sigidi. Molecular spectroscopic (ftir and uv-vis) and hyphenated chromatographic (uhplc-qtof-ms) analysis and in vitro bioactivities of the momordica balsamina leaf extract. *Biochemistry Research International*, 2021(1):854217, 2021.

[48] G.D.S. Grasel, M.F. Ferrão, and C.R. Wolf. Ultraviolet spectroscopy and chemometrics for the identification of vegetable tannins. *Industrial Crops and Products*, 91:279–285, 2016.

[49] T.K. Patle, K. Shrivas, R. Kurrey, S. Upadhyay, R. Jangde, and R. Chauhan. Phytochemical screening and determination of phenolics and flavonoids in dillenia pentagyna using uv-vis and ftir spectroscopy. *Spectrochimica Acta Part A: Molecular and Biomolecular Spectroscopy*, 242:118717, 2020.

[50] R. Verma, K. Akanksha, S.K. Jha, and L. Rani. Comparative studies of functional groups present in invasive and economically important plant leaf methanolic extracts by using ftir spectroscopic analysis. *Green and Sustainable Chemistry*, 23(3):184–191, 2023.

[51] A. Sulistiawan, W. Setyaningsih, and A. Rohman. A new ftir method combined with multivariate data analysis for determining aflatoxins in peanuts (arachis hypogaea). *Journal of Applied Pharmaceutical Science*, 12(7):199–206, 2022.

[52] P.P. Yue, Y.J. Hu, G.O. Fu, C.X. Sun, M.F. Li, F. Peng, and R.C. Sun. Structural differences between the lignin-carbohydrate complexes (lccs) from 2- and 24-month old bamboo (neosinocalamus affinis). *International Journal of Molecular Sciences*, 19(1):1, 2018.

[53] J.M. Barcelo, A.M. Gatchallan, I.J.B. Aquino, D.R.E. Ollero, F.L.D. Cortez, T.M. Costales, and L.A.Q. Marzo. Ftir spectrum and antimutagenicity of coffea arabica pulp and arachis hypogaea test in relation to their in vitro antioxidant properties. *Asia Pacific Journal of Multidisciplinary Research*, 3(4):99–108, 2015.

[54] K.K. Veedu, T.P. Kalarikkal, N. Jayakumar, and N.K. Gopalan. Anticorrosive performance of mangifera indica l. leaf extract-based hybrid coating on steel. *ACS Omega*, 4(6):10176–10184, 2019.

[55] M. Maczka, A. Ciupa, A. Gągor, A. Sieradzki, A. Pikul, B. Macalik, and M. Drozd. Perovskite metal formate framework of [nh2-ch+-nh2]mn(hcoo)3]: Phase transition, magnetic, dielectric, and phonon properties. *Inorganic Chemistry*, 53(10):5260–5268, 2014.

[56] A.B.D. Nandiyanto, R. Ragadhita, and F. Fiandini. Interpretation of fourier transform infrared spectra (ftir): A practical approach in the polymer/plastic thermal decomposition. *Indonesian Journal of Science and Technology*, 8(1):113–126, 2023.

[57] V.S. Sastri. *Green Corrosion Inhibitors: Theory and Practice*. John Wiley & Sons, Inc., England, 1st edition, 2011.

[58] B. Kumar and L. Cumbal. Uv-vis, ftir and antioxidant study of persea americana (avocado) leaf and fruit: A comparison. *Revista de la Facultad de Ciencias Químicas*, 14:14, 2016.

[59] S. Sharma, A. Solanki, and S. Sharma. Anticorrosive action of eco-friendly plant extracts on mild steel in different concentrations of hydrochloric acid. *Corrosion Reviews*, 42(2), 2024.

[60] O. Okiemute, O. Richard, and E. Salif. Investigating the influence of immersion time and inhibitor concentration on the inhibiting potential of imperrata cylindrica as corrosion inhibitor of mild steel. *International Journal of Research in Engineering and Innovation*, 6(1):147–152, 2017.

[61] A.A.H. Al-Amiery, L.M. Shaker, A.A.H. Kadhum, and M.S. Takriff. Exploration of furan derivative for application as corrosion inhibitor for mild steel in hydrochloric acid solution: Effect of immersion time and temperature on efficiency. *Materials Today: Proceedings*, 42(5):2968–2973, 2021.

[62] S. Umoren, I. Obot, Z. Gasem, and N. Odemunmi. Experimental and theoretical studies of red apple fruit extracts as green corrosion inhibitor for mild steel in hcl solution. *Journal of Dispersion Science and Technology*, 36(6):782–802, 2015.

[63] K. Komalasari, S. Utami, M. Fermi, Y. Aziz, and I. Irianti. Corrosion control of carbon steel using inhibitor of banana peel extract in acid diluted solutions. In *IOP Conference Series: Materials Science and Engineering*, volume 345, page 012030, 2018.

[64] Q. Wang, C. Zhao, Q. Zhang, X. Zhou, Z. Yan, Y. Sun, D. Sun, and X. Li. Synergistic effect of benincasa hispida peel extract and ki on the corrosion inhibition of mild steel in hcl. *Sustainability*, 15(14):11370, 2023.

[65] A. Kokalj. On the use of the langmuir and other adsorption isotherms in corrosion inhibition. *Corrosion Science*, 217:111112, 2023.

[66] N. Bhardwaj, P. Sharma, and V. Kumar. Phytochemicals as steel corrosion inhibitor: An insight into mechanism. *Corrosion Reviews*, 39(1):27–42, 2021.

[67] M. Mamudu, M.S. Alnarabiji, and R.C. Lim. Adsorption isotherm and molecular modeling of phytoconstituents from dillenia suffruticosa leaves for corrosion inhibition of mild steel in 1.0 m hydrochloric acid solution. *Research on Surface Interfaces*, 13:100145, 2023.

[68] M. Amin, N. El-Bagoury, M. Saracoglu, and M. Ramadan. Electrochemical and corrosion behavior of cast re-containing inconel 718 alloys in sulfuric acid solutions and the effect of cl. *International Journal of Electrochemical Science*, 9(9):5352–5374, 2014.

[69] R.T. Loto. Electrochemical analysis of the corrosion inhibition effect of trypsin complex on the pitting corrosion of 420 martensitic stainless steel in 2m h2so4 solution. *PLoS One*, 13(4):e0195870, 2018.

[70] M. May. Corrosion behavior of mild steel immersed in different concentrations of nacl solutions. *Journal of Sebha University Pure and Applied Sciences*, 15:1–12, 2016.

[71] S. Congtao, S. Ming, J. Liu, L. Fan, and J. Duan. Anti-corrosion performance of migratory corrosion inhibitors on reinforced concrete

exposed to varying degrees of chloride erosion. *Materials*, 15(15):5138, 2022.

[72] D.K. Verma and F. Khan. Green approach to corrosion inhibition of mild steel in hydrochloric acid medium using extract of spirogyra algae. *Green Chemistry Letters and Reviews*, 9(1):52–60, 2016.

[73] C.K. Tao, Y.J. Wu, W.Y. Wang, Y.S. Qian, R. Tao, and T. Kang. Experimental investigation of white-light interferometry based on sub-dark-field illumination. *Optics Communications*, 435:108–117, 2019.

[74] Y. Wang, T. Wang, B. Wang, W. Chang, J. Cao, L. Hu, M. Lu, and L. Zhang. Performance evaluation of a novel and effective water-soluble aldehydes as corrosion inhibitor for carbon steel in aggressive hydrochloric medium. *Journal of Renewable Materials*, 10(2):301–327, 2022.

[75] B.R. Fazal, T. Becker, B. Kinsella, and K. Lepkova. A review of plant extracts as green corrosion inhibitors for co2 corrosion of carbon steel. *npj Materials Degradation*, 6(5):1–14, 2022.